OncoTargets and Therapy

Dovepress
open access to scientific and medical research

Open Access Full Text Article

ORIGINAL RESEARCH

RETRACTED ARTICLE: KDM5C Expedites Lung Cancer Growth and Metastasis Through Epigenetic Regulation of MicroRNA-133a

This article was published in the following Dove Press journal:
OncoTargets and Therapy

Quan Zhang*
Lei Xu*
Jianjun Wang
Xiaoming Zhu
Zeheng Ma
Junfeng Yang
Jiwei Li
Xiangbo Jia
Li Wei

Department of Thoracic Surgery, Zhengzhou Key Laboratory of Surgical Treatment for End-Stage Lung Diseases, Henan Provincial People's Hospital, People's Hospital of Zhengzhou University, Zhengzhou, 450003, Henan, People's Republic of China

*These authors contributed equally to this work

Background: KDM5C, a histone H3K4-specific demethylase, possesses various biological functions in development of cancers. However, its relation to the microRNA (miRNA) regulation in lung cancer remains unknown. This study aims to study the regulatory role of KDM5C on modification of miR-133a in the progression of lung cancer.

Methods: Differentially expressed miRNAs were filtered from 34 paired lung cancer and paracancerous tissues. The correlation between miR-133a expression and the prognosis of lung cancer patients was determined by a bioinformatics website. Furthermore, malignant aggressiveness of lung cancer cells was detected after miR-133a upregulation by CCK-8, flow cytometry, and Transwell assays and in vivo tumorigenesis and metastasis experiments. Subsequently, we analyzed mRNA downregulated in cells overexpressing miR-133a using microarray analysis and expounded the upstream regulatory mechanism of miR-133a using bioinformatics website prediction and functional validation.

Results: miR-133a was reduced in lung cancer tissues, and patients with low expression of miR-133a had worse survival rates. miR-133a restoration curtailed growth and metastasis of lung cancer cells in vitro and in vivo. Moreover, miR-133a downregulated PTBP1 expression, whereas overexpression of PTBP1 attenuated the suppressive effect of miR-133a on lung cancer cell aggressiveness. The level of methylation modification of miR-133a was reduced in lung cancer cells. KDM5C inhibited the expression of miR-133a by promoting the demethylation modification of its promoter histone.

Conclusion: Histone demethylase KDM5C inhibits the expression of miR-133a by elevating the demethylation modification of the promoter histone of miR-133a, thereby promoting the expression of PTBP1, which finally accelerates lung cancer cell growth and metastasis.

Keywords: KDM5C, microRNA-133a, lung cancer, PTBP1, histone methylation modification

Introduction

In the last century, lung cancer has progressed from an infrequent and obscure disease towards the most frequent malignancy in the world and the leading cause of death from cancer,[1] accounting for 11.6% of the total diagnoses and 18.4% of the total deaths related to cancers in 2018 worldwide.[2] Lung cancer is classified into two main categories: non-small cell lung carcinoma (85% of new lung cancer diagnoses), which can further be allocated into lung adenocarcinoma (LUAD), lung squamous-cell carcinoma (LUSC), and large-cell carcinoma, as well as small-cell lung carcinoma (15% of new lung cancer diagnoses).[3] Notable

Correspondence: Li Wei
Department of Thoracic Surgery, Zhengzhou Key Laboratory of Surgical Treatment for End-Stage Lung Diseases, Henan Provincial People's Hospital, People's Hospital of Zhengzhou University, No. 7, Weiwu Road, Jinshui District, Zhengzhou, 450003, Henan, People's Republic of China
Tel/Fax +86-18339223972
Email Liwei71710@163.com

declines in mortality from lung cancer have been witnessed thanks to incidence reduction because of smoking cessation and decreasing rates of smoking uptake, and further reductions in mortality might be accomplished through treatment, particularly if the disease is diagnosed at an early stage when curative therapy is possible.[4] Therefore, it is of paramount importance to elucidate the mechanisms underlying lung cancer development and to identify novel prognostic biomarkers and therapeutic target options for improving the diagnosis and treatment.

MicroRNAs (miRNAs) are a big family of post-transcriptional mediators of gene expression which are about 21 nucleotides in length and govern many developmental and cellular events.[5] Moreover, miRNAs are inclined to be localized in fragile chromosomal regions which are prone to deletions, translocations and amplifications and are frequently altered in different cancers.[6] Among them, a comprehensive study based on meta-analysis and The Cancer Genome Atlas (TCGA) database revealed that miR-133a is significantly lower in lung cancer tissues than in normal tissues, making it an independent prognostic and diagnostic biomarker for non-small cell lung cancers.[7] In addition, miR-133a has also been revealed to exhibit tumor suppressive roles by targeting different mRNAs in lung cancer.[8,9] However, the upstream mechanism of miR-133a in lung cancer is gaining more interests. For instance, Cryptotanshinone, a natural quinoid diterpene, has been reported to inhibit lung cancer invasion by upregulating miR-133a.[10] From the perspective of molecular mechanism, lysine methylation is one of the histone posttranslational modifications that alters chromatin structure, and alterations in histone lysine methylation have been implicated in cancer formation, which is believed as a consequence of the dysregulation of histone lysine methyltransferases or the demethylases.[11] Although the lysine demethylase 5 (KDM5) demethylases act as oncogets in cancer, KDM5C, a gene not inactivated on the X chromosome, was relatively less studied relative to its counterparts KDM5A, KDM5B and KDM5D.[12] In this investigation, we expounded the regulation of KDM5C on miR-133a during lung cancer progression and further studied the potential downstream target of miR-133a.

Materials and Methods

Clinical Samples and Follow-Up Studies

Tumor tissues and the corresponding adjacent tissues were collected from 37 patients with lung cancer in People's Hospital of Zhengzhou University. All participants did not receive preoperative chemotherapy, radiation, or other anti-cancer therapy before enrollment. Immediately after surgical excision, the tissues were immersed in liquid nitrogen and kept in liquid nitrogen until use. We obtained the written informed consent from each participant before surgery. The Research Ethics Committee of People's Hospital of Zhengzhou University approved the study protocol. The study was implemented in compliance with the ethical guidelines of the 1975 Declaration of Helsinki.

miRNA-Based Microarray

Total RNA was isolated from tissues or A549 and H1299 cells after transfection with the help of TRIzol reagent (Invitrogen Inc., Carlsbad, CA, USA). Total RNA concentration and purity were assessed using a NanoDrop ND-2000 (Thermo Fisher Scientific Inc., Waltham, MA, USA), and RNA integrity was verified using an Agilent 2100 Bioanalyzer (Agilent Technologies, Santa Clara, CA, USA). Total RNA was dephosphorylated, denatured, and labeled with cyanine-3-CTP. Oebiotech (Shanghai, China) was commissioned to perform miRNA microarray assays. Labeled RNA samples were competitively hybridized to microarray (Agilent Human miRNA microarray, Design ID: 070156). After being washed, the microarray was scanned with an Agilent scanner G2505C (Agilent Technologies).

Analysis of Public Databases

StarBase bioinformatics prediction website (http://starbase.sysu.edu.cn/) was utilized to predict target mRNAs of miR-133a. miR-133a was found to be located on chromosome 18 at chr18:21825698–21825785 using the UCSC (http://bio.lundberg.gu.se/courses/vt13/ucsc.html) website. The correlation of KDM5C with miR-133a or PTBP1 was analyzed in TCGA-LUAD database (https://cancergenome.nih.gov/). The staining intensity of six genes, including PTPB1, SP1, ANXA5, DUSP1, LDLR and NME4, was analyzed in lung cancer or normal lung tissues via the HPA website (https://www.proteinatlas.org/). Expression of PTP1B in a variety of cancer tissues and cells were analyzed by the CCLE database (https://portals.broadinstitute.org/ccle/about). PTBP1 and KDM5C expression profiles were detected using the Oncomine database (https://www.oncomine.org/) in Garber Lung,[13] Hou Lung,[14] Okayama Lung,[15] Selamat Lung,[16] Stearman Lung,[16] and Talbot Lung.[17]

Reverse Transcription Quantitative PCR (RT-qPCR)

Following total RNA extraction using TRIzol reagent (Invitrogen), cDNA was synthesized using Mir-X miRNA First-Strand Synthesis Kit (Takara Holdings Inc., Kyoto, Japan) with extracted total RNA (2 μg). The miRNA expression was measured by qPCR with SYBR Advantage qPCR Premix (Takara) on CFX133a Real-Time PCR Detection System (Bio-Rad Laboratories, Hercules, CA, USA). Relative expression was determined with a U6 control through the $2^{-\Delta\Delta Ct}$ method. The primers used are depicted in Table 1.

Cell Culture, Transfection and Infection

Human lung cancer cell lines, including H522, H460, SK-MES-1, and A549, and a human bronchial epithelial cell line BEAS-2B, were from the Institute of Biochemistry and Cell Biology, Chinese Academy of Sciences (Shanghai, China). Cell lines H522, H460, and A549 were cultivated in RPMI-1640 medium (Gibco; Thermo Fisher Scientific), while SK-MES-1 cells were in minimal medium (Gibco). Both media contained 10% FBS (Gibco) and 1% penicillin-streptomycin mixture (Gibco). BEAS-2B cells were exposed to bronchial epithelial growth medium (Lonza/Clonetics, Walkersville, MD, USA) containing 0.5 ng/mL epidermal growth factor, 500 ng/mL hydrocortisone, 0.25 ng/mL bovine pituitary extract, 500 mM ethanolamine, 500 mM ethanolamine phosphate, 0.01 mg/mL epinephrine, and 0.1 g/mL retinoic acid. All cells were maintained at 37°C in the presence of 5% CO2.

The synthesized miR-133a mimic and negative control (NC) mimic (GenePharma, Shanghai, China) were resuspended in 20 μM diethyl pyrocarbonate water. Briefly, NC mimic, miR-133a mimic, and Lipofectamine 3000 (Invitrogen) were each diluted with 100 μL serum-free medium. The diluted Lipofectamine 3000 was added to the diluted NC mimic or miR-133a mimic, respectively, and incubated at ambient temperature for 30 min. The mixture was subsequently added to cell suspensions of A549 and H1299. Subsequently, A549 and H1299 cells stably overexpressing miR-133a were infected with lentiviral vectors of overexpression (oe)-NC, oe-PTBP1 or oe-KDM5C for 2 days. The expression of miR-133a, PTBP1, and KDM5C in cells were verified using RT-qPCR or Western blot to confirm successful infection/transfection of the cells.

Cell Viability Assay

The viability of lung cancer cells was evaluated using cell counting kit-8 (CCK-8, Beyotime, Shanghai, China). Lung cancer cells were plated into 96-well plates and cultured at 37°C in an incubator for 24, 48, and 72 h. A total of 10 μL CCK8 reagent was loaded onto each well, and cells were cultured for another 3 h. The optical density (OD) value at 450 nm was detected to assess the cell viability.

Flow Cytometric Analysis

The cells were detached with 0.25% trypsin (90058, Thermo Scientific). After detachment, 100 μL binding buffer was added to prepare cell suspension (1×10^6 cells/mL). Annexin V-fluorescein isothiocyanate (FITC, 40302ES20,

Table 1 Primer Sequences

Targets	Forward (5′-3′)	Reverse (5′-3′)
miR-133a	TTTGGTCCCCTTCAACC	GAACATGTCTGCGTATCTC
miR-376b	TCATAGAGGAAAATCCATG	GAACATGTCTGCGTATCTC
miR-103	CAGCATTGTACAGGGCT	GAACATGTCTGCGTATCTC
miR-410	TATAACACAGATGGCCTG	GAACATGTCTGCGTATCTC
miR-720	TCTCGCTGGGGCCTC	GAACATGTCTGCGTATCTC
miR-1914	TGTAACAGCAACTCCATGTG	GAACATGTCTGCGTATCTC
miR-135	TGGCTTTTTATTCCTATGTG	GAACATGTCTGCGTATCTC
miR-1226	GTGAGGGCATGCAGGC	GAACATGTCTGCGTATCTC
miR-107	CAGCATTGTACAGGGCT	GAACATGTCTGCGTATCTC
miR-379	TGGTAGACTATGGAACGT	GAACATGTCTGCGTATCTC
U6	CTCGCTTCGGCAGCACAT	TTTGCGTGTCATCCTTGCG
PTP1B	TGTCTGGCTGATACCTGCCTCT	ATCAGCCCCATCCGAAACTTCC
KDM5C	ACTGCTGACCATTGCTGAACGC	CCTCCTTGAGAGCCTGGATGTT
GAPDH	GTCTCCTCTGACTTCAACAGCG	ACCACCCTGTTGCTGTAGCCAA

Abbreviations: miR, microRNA; KDM5C, lysine-specific histone demethylase 5C; PTBP1, polypyrimidine tract-binding protein 1; GAPDH, glyceraldehyde-3-phosphate dehydrogenase.

Yeasen Biotechnology Co., Ltd., Shanghai, China) and propidium iodide (PI) were added sequentially for a 5-min incubation in darkness at ambient temperature. The FC500MCL flow cytometer (FACS Canto II, BD Biosciences, San Jose, CA, USA) system was applied to assess apoptosis.

Transwell Assays

Cell migration and invasion were examined by Transwell assays. In Transwell invasion assay, porous membranes were pre-coated with Matrigel (BD Biosciences). A549 and H1299 cells suspended in serum-free medium (200 μL) was transferred to the pre-coated apical chamber. The basolateral chamber was added with 500 μL medium plus 10% FBS. After 24 h of incubation, cells left on the upper side of the membrane were removed. Invasive cells were stained with crystal violet. Cells in the five random fields were counted using a microscope. Migration assay was performed using uncoated apical chambers according to a similar protocol.

In vivo Tumorigenesis Experiments

All experiments regarding animals were implemented with the approval of the Animal Care and Use Committee of People's Hospital of Zhengzhou University. The report of animal experiments is in compliance with the Guide for the Care and Use of Laboratory animals published by the US National Institutes of Health. Adequate measures were taken to minimize the number of rats used and to ensure no pain or discomfort. Twenty-four immunodeficient mice (male, 5 weeks, Hunan SJA Laboratory Animal Co., Ltd., Changsha, Hunan, China) were reared in SPF grade environment. Lung cancer cells overexpressing miR-133a were resuspended in phosphate-buffered saline (2×10^6 cells/mL) and mixed with Matrigel (1:1). The mixture (0.1 mL) was injected subcutaneously into the flanks of the mouse. Tumor volume was tested every 5 d with vernier calipers using the equation: $V = 1/2 \times a \times b^2$. After 5 weeks and mouse euthanasia, the tumors were harvested and weighed. Tumor samples were evaluated histologically.

Immunohistochemistry

The excised tumor tissues were dehydrated by formalin, paraffin-embedded, and cut into 4-μm thickness sections. The sections were dewaxed, rehydrated, and microwaved to remove antigen. The activity of endogenous peroxidase was eliminated using H_2O_2 (3%). After a 20 min treatment in 5% BSA (A1128; Gentihold, Beijing, China), the sections were subjected to an overnight incubation with primary antibody (1:200) at 4°C, and a 1-h incubation with biotinylated secondary antibody (1:500) at 37°C. The sections were then stained with diaminobenzidine, counterstained with hematoxylin and incubated in alcohol and xylene. An inverted fluorescence microscope (Olympus Optical Co., Ltd., Tokyo, Japan) was used for visualization in five random fields (400×). Stained cells were calculated, and positive staining rates were analyzed by Image J.

Terminal Deoxynucleotidyl Transferase (TdT)-Mediated dUTP-Biotin Nick End Labeling (TUNEL)

Tumor tissue sections were routinely dewaxed, rehydrated and tested according to the TUNEL assay conforming to the manufacturer's instructions (Roche Diagnostics, Co., Ltd., Rotkreuz, Switzerland). Briefly, sections were first incubated in a TdT reaction cocktail for 45 min at 37°C, followed by treatment with a Click-iT reaction cocktail. Hematoxylin was applied for nuclei staining.

Tail Vein Metastasis Model in vivo

Twenty-four male immunodeficient mice (5 weeks of age) were reared in specific-pathogen-free grade environment. Cells overexpressing miR-133a (2×10^7) were injected into the tail vein of nude mice. After 45 d, mice were euthanized by overdose pentobarbital sodium. Liver and lung tissues were surgically removed and fixed in formalin for further analysis.

Hematoxylin-Eosin (HE) Staining

The liver and lung tissues were fixed in 4% paraformaldehyde (BOSTER, Wuhan, Hubei, China) for 2 d at ambient temperature, dehydrated in a graded series of alcohols, washed in xylene, and paraffin-embedded. A rotating microscope knife was used to cut the paraffin block into 4-μm sections. Sections were de-paraffinized and stained with HE. Stained tissue sections were examined using an optical microscope (Olympus).

Dual-Luciferase Assays

Prediction of interactions between miR-133a and PTBP1 3′untranslated region (3′UTR) was conducted via the StarBase bioinformatics prediction website (http://star

base.sysu.edu.cn/). The sequences of PTBP1 3′UTR wild-type (wt) or mutant (mt) were constructed by GenScript (Nanjing, Jiangsu, China). Cells were transfected with miR-133a mimic and PTBP1 3′UTR (wt) or PTBP1 3′UTR (mt) with the help of Lipofectamine 2000 (Invitrogen). After 48 h, luciferase activity was assessed using the dual-luciferase reporter assay system (Promega Corporation, Madison, WI, USA). Firefly luciferase activity was normalized to Renilla luciferase activity.

RNA Immunoprecipitation (RIP)

A Magna RNA-binding protein immunoprecipitation kit (Invitrogen) was applied in this experiment as per the protocol provided by the manufacturer. Lysates in RIP buffer were co-cultured with magnetic beads containing anti-IgG (NC) or anti-Ago2. Afterwards, the immunoprecipitated RNAs were assessed by RT-qPCR.

Chromatin Immunoprecipitation (ChIP)

ChIP-qPCR assays were conducted as per standard protocols. Briefly, the cross-linked cell lysates were sonicated and subjected to immunoprecipitation reactions. Immunoprecipitated DNA was purified using the universal DNA purification kit (TIANGEN Biotech Co., Ltd., Beijing, China). One percent of each sample volume was taken as "input", separately. KDM5C antibody (1:40, as applied as the primary antibody (Abcam, Cambridge, MA, USA). Purified DNA was analyzed by qPCR.

Statistics

SPSS version 22.0 (IBM Corp. Armonk, N.Y., USA) was applied for statistical analysis. The data was displayed as mean ± standard deviation (SD) and analyzed using paired *t* test, one-way or two-way analysis of variance (ANOVA) followed by Tukey's post hoc test. Difference at *p*-value < 0.05 was considered significant.

Results

miR-133a is Poorly Expressed in Lung Cancer Patients and Correlates with Dismal Prognosis

We first analyzed the differentially expressed miRNAs in 37 lung cancer tissues and paracancerous tissues using miRNA-based microarray. Using the R Limma package, with screening thresholds set at |Log Fold Change > 2| and *p* value < 0.05, we screened 368 differentially expressed miRNAs, of which 97 miRNAs were significantly downregulated and 271 were upregulated (Figure 1A). The heatmap shows the top 100 differentially expressed miRNAs (Figure 1B). Table 2 shows the top 60 differentially expressed miRNAs. We further used RT-qPCR to measure the expression of the top ten differentially expressed miRNAs in lung cancer tissues and paracancerous tissues. miR-133a was revealed as the most significantly downregulated one in lung cancer tissues (75.43 ± 5.97%) (Figure 1C). We observed that miR-133a was significantly under-expressed in TCGA-LUAD and TCGA-lung squamous cell carcinoma (LUSC) (Figure 1D and E). We then analyzed miR-133a via the Kaplan-Meier Plotter website and found that lung cancer patients with higher expression of miR-133a had prolonged survival period (Figure 1F). We further examined the miR-133a expression profile in BEAS-2B cells and lung cancer cells. miR-133a expression was notably reduced in H1299 (77.13 ± 9.42%) and A549 (68.15 ± 7.64%) cells (Figure 1G). Thus, we speculated that miR-133a may have the ability to act as a tumor suppressor in lung cancer.

Overexpression of miR-133a Inhibits the Growth and Aggressiveness of Lung Cancer Cells in vitro

To further validate the tumor suppressive effect of miR-133a, we transfected miR-133a mimic (Figure 2A) in A549 and H1299 cells. First, we assayed the proliferative activity of cells using the CCK-8 assay. Significant declines were observed in cell activity of A549 and H1299 after miR-133a mimic transfection (Figure 2B). Among the three indicated time points, the cellular activities of A549 and H1299 decreased by 20.51 ± 2.43% and 19.76 ± 1.85% at the 24th h, 70.42 ± 6.91% and 66.39 ± 6.53% at the 48th h, and at the 72nd h, the cellular activities of A549 and H1299 decreased by 69.42 ± 7.68% and 63.66 ± 6.59%. Moreover, we further used flow cytometry to detect apoptosis rate and found that miR-133a significantly promoted a significant increase in PI^+ Annexin-V^+ and PI^- Annexin V^+ cells (Figure 2C). The total number of apoptotic cells in A549 cells elevated from 8.14 ± 0.82% to 26.45 ± 2.65% and in H1299 cells increased from 6.93 ± 0.71% to 23.91 ± 2.36% after

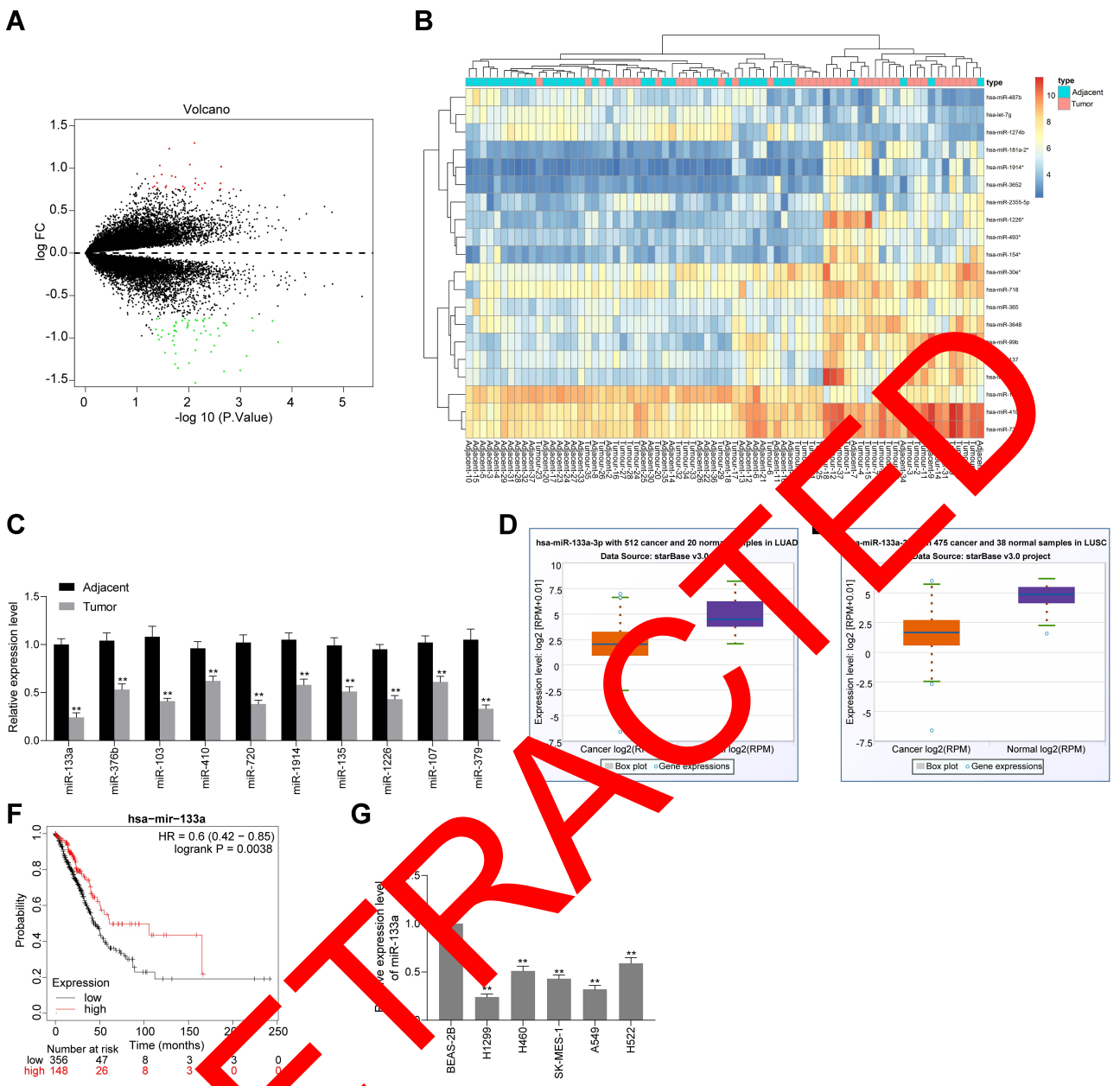

Figure 1 miR-133a is t[illegible] in lung [illegible]cer patie[illegible] and correlates with unsatisfactory prognosis. (**A**) the volcano map showing differentially expressed miRNAs in lung cancer tissues and [illegible]acancer[illegible]s tissues; (**B**) th[illegible] heatmap showing the top 100 differentially expressed miRNAs; (**C**) RT-qPCR detection of expression of the top ten miRNAs in 37 pai[illegible]d lung canc[illegible] tissues and p[illegible]acancerous tissues; (**D**) miR-133a expression in the TCGA-LUAD database; (**E**) expression of miR-133a in the TCGA-LUSC database; (**F**) Ka[illegible]-Meier P[illegible]ote analyzing the correlation between miR-133a and survival in lung cancer patients; (**G**) expression of miR-133a in BEAS-2B cells and lung cancer cells by [illegible]R. Data are presented as the mean ± SD. $^{**}p < 0.01$. All results are from three independent experiment. Paired *t* test was applied for two-sample comparisons (**C**), whi[illegible]e-way ANOVA followed by Tukey post hoc test was utilized for multiple comparisons (**G**).

Abbreviations: hsa, *Ho[illegible]sapiens*; miR, microRNA; TCGA, The Cancer Genome Atlas; LUAD, lung adenocarcinoma; LUSC, lung squamous cell carcinoma; RT-qPCR, reverse transcription quantit[illegible]e PCR; ANOVA, analysis of variance; SD, standard deviation.

overexpression of miR-133a. Transwell experiments were then performed to assess the effect of miR-133a on the aggressiveness of lung cancer cells, and we found that A549 and H1299 cells with miR-133a mimic had a remarkable reduction in the number of cells migrated and invaded into the basolateral chamber (Figure 2D and E). In A549 cells, the number of migrated cells reduced from 136.25 ± 15.42 to 41.74 ± 5.26 and the number of invaded cells decreased from 96.55 ± 8.57 to 35.38 ± 4.19 after overexpression of miR-133a. In H1299 cells, the number of migrated cells diminished from 158.97 ± 16.23 to 53.36 ± 7.48, while the number

Table 2 Differentially Expressed miRNAs Between Lung Cancer Tissues and Normal Lung Tissues

Targets	Log Fold Change	*p* value	Targets	Log Fold Change	*p* value
hsa-miR-30e*	−1.05	0.000186192**	hsa-miR-498	−0.79	0.006897349**
hsa-miR-365	−0.8	0.000237485**	hsa-miR-3127	−1.02	0.007062561**
hsa-miR-410	−0.91	0.000578197**	hsa-miR-125a-3p	−0.79	0.007368496**
hsa-miR-493*	−0.76	0.000589149**	hsa-miR-452	0.88	0.007387207**
hsa-miR-1914*	−1.21	0.000760287**	hsa-miR-335	0.82	0.007422249**
hsa-miR-1226*	−1.38	0.001001076**	hsa-miR-149	−1.15	0.007425284**
hsa-let-7g	0.75	0.00136076**	hsa-miR-543	−1.53	0.007445407**
hsa-miR-3652	−0.85	0.001867851**	hsa-miR-3937	−1.58	0.00745166**
hsa-miR-718	−0.83	0.001977127**	hsa-miR-181d	0.75	0.007594213**
hsa-miR-133a	−1.39	0.002064881**	hsa-miR-371-5p	1.3	0.007709963**
hsa-miR-720	−0.82	0.002141302**	hsa-miR-23a*	−0.91	0.007935064**
hsa-miR-1274b	1.02	0.002356211**	hsa-miR-409-3p	1.04	0.00952764**
hsa-miR-487b	0.82	0.002410418**	hsa-miR-125b-2*	−1	0.009867288**
hsa-miR-103	0.75	0.002431426**	hsa-miR-1225-3p	0.8	0.009889021**
hsa-miR-181a-2*	−0.98	0.002583682**	hsa-miR-187*	−0.86	0.010380745**
hsa-miR-137	−0.89	0.002721293**	hsa-miR-3137	−0	0.010433333**
hsa-miR-154*	−1.09	0.003207005**	hsa-miR-454	35	0.010535843**
hsa-miR-200b*	−1.16	0.003698269**	hsa-miR-4	−0.8	0.010706312**
hsa-miR-3648	−0.96	0.003803141**	hsa-miR-210	−0.77	0.011910802**
hsa-miR-2355-5p	−0.77	0.004010746**	hsa-miR-193a-5p	0.77	0.011969383**
hsa-miR-575	−0.92	0.004718477**	hsa-miR-548c-3p	0.79	0.012915799**
hsa-miR-299-5p	0.82	0.004861099**	hsa-miR-548c	−0.8	0.013351085**
hsa-miR-379	−0.77	0.004938248**	hsa-miR-373*	−1.35	0.016161197**
hsa-miR-549-3p	−0.86	0.005070784**	hsa-miR-427	−0.92	0.017476469**
hsa-miR-107	−0.8	0.005214	hsa-miR-198	−0.91	0.018544204**
hsa-miR-200a*	−0.79	0.005244	hsa-miR-4322	−0.86	0.018802218**
hsa-miR-30c	0.76	0.005524125	hsa-miR-224*	−0.91	0.01898823**
hsa-miR-135a*	−0.95	0.0 757253	hsa-miR-200c*	−1.08	0.019046734**

Abbreviations: hsa, *Homo sapiens*; miRNA, microR **p < 0.0

of invading cells decreased om 129.2 ± 11.12 to 45.63 ± 4.15. The above results tatively suggest that miR-133a inhibits th growth and ggressiveness of lung cancer cells i vitro.

miR-133a Upreg lation Hampers the Growth and Metas sis in Lung Cancer

A549 a H12 bly overexpressing miR-133a or mimic cont were implanted into the axilla of nude mice by subcutaneous i ction. The volume of the xenograft tumor was measured every 5 days from 5 days after implantation to assess its growth rate. We found that mice injected with A549 or H1299 cells overexpressing miR-133a showed significantly reduced tumor growth rates in vivo. At day 35, the volume and weight of xenograft tumors formed by A549 cells overexpressing miR-133a decreased by 43.17 ± 5.22% and 46.17 ± 3.73%, respectively compared to those formed by cells expressing mimic NC, while the volume and weight of xenograft tumors formed by H1299 cells after overexpression of miR-133a decreased by 40.55 ± 5.04% and 39.63 ± 3.81%, respectively (Figure 3A–C). Furthermore, the positive rate of KI67 decreased by 55.04 ± 4.83% after overexpression of miR-133a in A549-forming xenograft tumors, while the positive rate of TUNEL increased from 5.47 ± 0.56% to 17.43 ± 1.82%. Consistently, the positive rate of KI67 after overexpression of miR-133a in xenograft tumors formed by H1299 decreased by 52.32 ± 5.64%, and the positive rate of TUNEL increased from 4.19 ± 0.42% to 15.37 ± 1.54% (Figure 3D and E). Subsequently, A549 and H1299 cells stably overexpressing miR-133a or mimic control were injected into mice via the tail vein to assess the effects of miR-133a on lung cancer metastasis in vivo. Forty-five days after inoculation, we extracted liver and lung tissues from mice after death and used HE staining to detect the

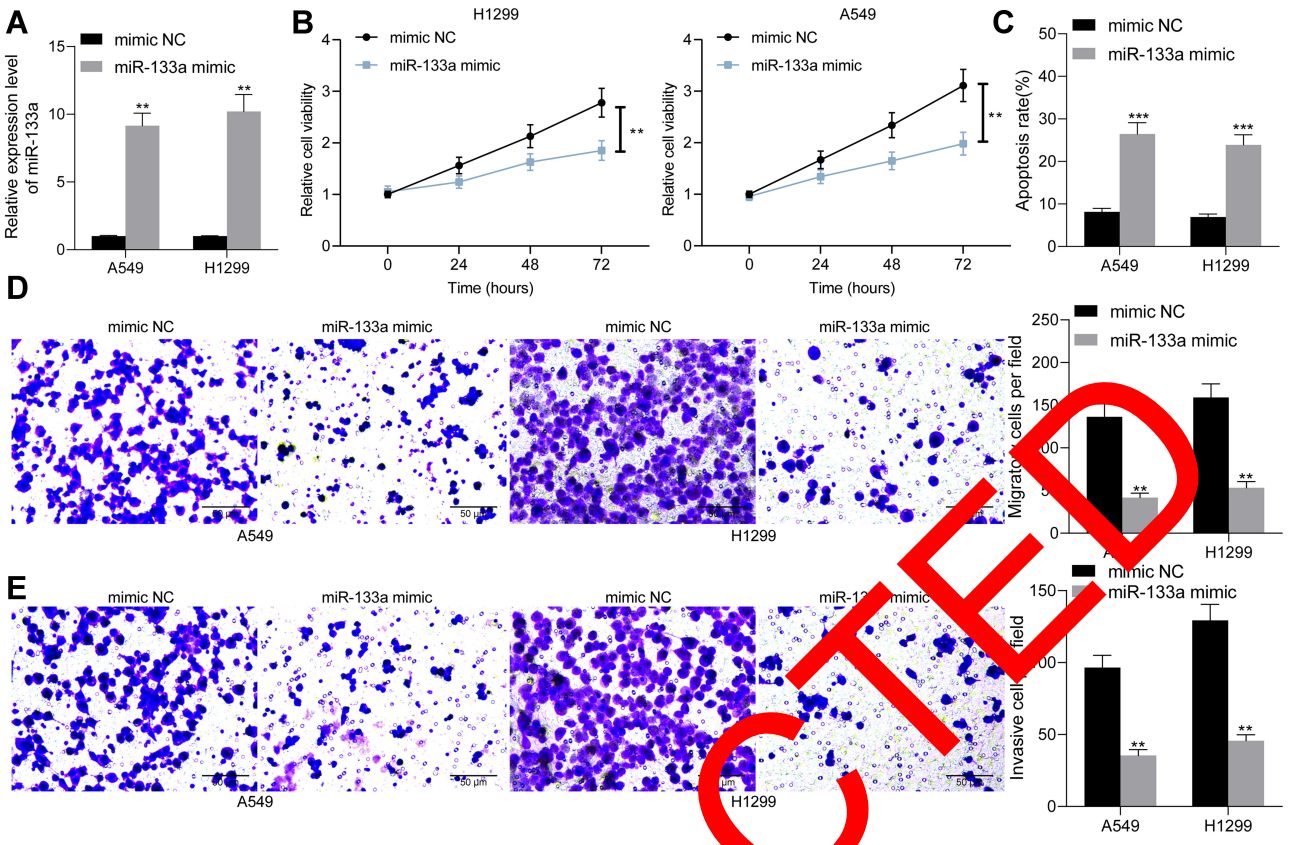

Figure 2 miR-133a upregulation hampers the viability and aggressiveness of lung cancer cells. miR-133a mimic or mimic control was transfected into A549 and H1299 cells. (**A**) RT-qPCR detection of miR-133a expression in lung cancer cells A549 and H1299 after transfection; (**B**) CCK-8 assays for cell proliferation activity; (**C**) flow cytometry analysis of apoptotic proportions of cells; (**D**) Transwell analysis of the migratory capacity of lung cancer cells; (**E**) Transwell analysis of the invasive capacity of lung cancer cells. Data are presented as the mean ± SD. $^{**}p < 0.01$, $^{***}p < 0.001$. The results are from three independent experiment. Two-way ANOVA followed by Tukey post hoc test was utilized for multiple comparisons.

Abbreviations: miR, microRNA; RT-qPCR, reverse transcription quantitative PCR; CCK-8, cell counting kit-8; ANOVA, analysis of variance; SD, standard deviation.

number of metastatic nodules. The results displayed that the number of metastatic nodules formed by A549 cells in lung tissues decreased from 12.74 ± 1.22 to 3.20 ± 0.33, in liver tissues from 10.46 ± 1.19 to 2.39 ± 0.28, and the number of metastatic nodules formed by H1299 cells in lung tissues decreased from 14.07 ± 1.41 to 5.12 ± 0.48 and in liver tissue decreased from 13.09 ± 1.27 to 3.11 ± 0.36 (Figure 3F and G).

miR-133a Targets the Negatively Regulates PTBP1

To clarify the downstream mechanism of miR-133a, we further employed microarray analysis to screen out differentially expressed mRNAs in A549 and H1299 cells with overexpression of miR-133a. Totally 344 genes were found to be significantly differentially expressed, of which 186 were significantly downregulated (Figure 4A). Table 3 shows the top 60 differentially expressed mRNAs. Subsequently, we further used the StarBase bioinformatics prediction website to predict target mRNAs for miR-133a and intersected with 186 downregulated genes with six genes, including PTPB1, SP1, ANXA5, DUSP1, LDLR, and NME4 in the intersection (Figure 4B). We then analyzed the staining intensity of these six genes in lung cancer or normal lung tissues via the HPA website, and we found that PTBP1 had the highest staining intensity in lung cancer tissue (Figure 4C). No significant difference in the expression of these six genes was found between lung cancer tissues and paracancerous tissues in the TCGA-LUSC database (Figure 4D). We then used the Kaplan-Meier Plotter website in order to further analyze the impact of these six genes on the prognosis of lung cancer patients.

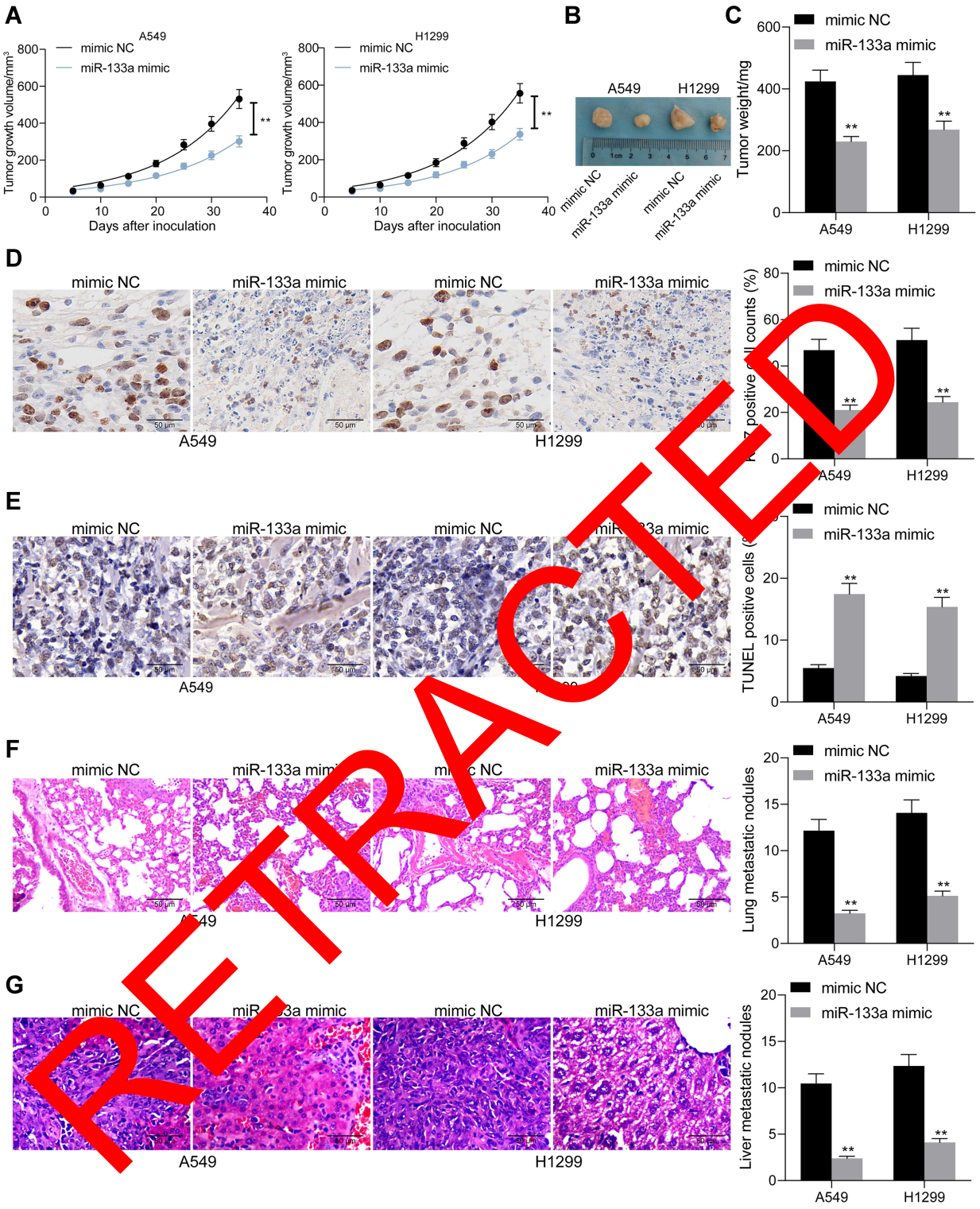

Figure 3 miR-133a upregulation suppresses the growth and metastasis of lung cancer. A549 and H1299 cells stably overexpressing miR-133a or mimic control were administrated into the axilla of mice by a subcutaneous injection. (**A**) volume growth rate of tumors; (**B**) representative tumor images; (**C**) tumor weight; (**D**) immunohistochemical detection of KI67-positive cells in tumor tissues; (**E**) TUNEL staining detection of the proportion of apoptotic cells in xenograft tumors. Similarly, A549 and H1299 cells stably overexpressing miR-133a or mimic control were injected into mice through the tail vein. (**F**) HE staining for the number of metastatic nodules in lung tissues of mice; (**G**) HE staining for the number of metastatic nodules in liver tissues of mice. Data are presented as the mean ± SD. $^{**}p < 0.01$. All results are from three independent experiment. Two-way ANOVA followed by Tukey post hoc test was utilized for multiple comparisons.

Abbreviations: miR, microRNA; TUNEL, terminal deoxynucleotidyl transferase (TdT)-mediated dUTP-biotin nick end labeling; HE, hematoxylin-eosin; ANOVA, analysis of variance; SD, standard deviation.

Only PTBP1 and SP1 showed significant influence on the prognosis of lung cancer patients (Figure 4E). To further clarify the targeting mechanism of miR-133a with SP1 or with PTBP1, we further analyzed the correlation between miR-133a and SP1 or PTBP1 in the TCGA-LUAD database, and we found that miR-133a had a significant correlation with PTBP1 and a poor correlation with SP1 (Figure 4F). Moreover, PTBP1 expression was observed to be significantly higher in lung cancer cells than in other cancer cells (Figure 4G) through the CCLE database. Thus, we retrieved PTBP1 expression in lung cancer tissues as well as in corresponding normal tissues using the Oncomine database. We found a significant increase in the expression of PTBP1 in lung cancer tissues relative to normal paracancerous tissues in the Garber Lung,[13] Hou Lung,[14] Okayama Lung,[15] Selamat Lung,[16] Stearman Lung,[16] and Talbot Lung[17] datasets (Figure 4H). To determine the possible binding relationship between miR-133a and PTBP1, we performed RIP experiments using an antibody against Ago2 in A549 and H1299 cells, and noted that more PTBP1 could be enriched in cells with miR-133a mimic (Figure 4I). We further performed dual-luciferase experiments and noted that in 293T cells with miR-133a mimic, only cells co-transfected with PTBP1-wt had a significant decline in luciferase activity, whereas no significant difference in luciferase activity was observed in cells with PTBP1-mt (Figure 4J and K). We further examined the mRNA and protein expression of PTBP1 in A549 and H1299 cells overexpressing miR-133a using RT-qPCR and Western blot. After overexpression of miR-133a, PTBP1 mRNA level decreased by 69.41 ± 7.24% and protein expression reduced by 57.62 ± 6.07% in A549 cells. While in H1299 cells, PTBP1 mRNA level diminished by 60.73 ± 5.89% and protein expression decreased by 51.16 ± 5.27% (Figs 4L and M).

Overexpression of PTBP1 Promotes Growth and Aggressiveness of Lung Cancer Cells in vitro

To further determine whether miR-133a inhibits the malignant biological behavior of lung cancer cells by targeting PTBP1, we further overexpressed PTBP1 in cells overexpressing miR-133a (Figure 5A). We found that after overexpression of PTBP1, the cellular viability of A549 and H1299 increased by 17.78 ± 1.63% and 21.05 ± 2.32% at 24th h, by 46.88 ± 4.93% and 32.35 ± 3.41% at 48th h, and by 46.51 ± 5.11% and 39.90 ± 4.17% at 72nd h (Figure 5B). The number of early and late apoptotic cells was also significantly reduced from 27.16 ± 2.72% to 12.67 ± 1.28%, and from 24.08 ± 2.41% to 10.33 ± 1.06%, respectively for A549 and H1299 cells (Figure 5C). Transwell assays disclosed that the invasion and migration capacities of A549 and H1299 cells increased significantly after overexpression of PTBP1, as shown by increased number of cells in the basolateral chamber (Figure 5D and E). In A549 cells, the number of migrated cells increased from 59.57 ± 5.06 to 95.77 ± 9.11 and the number of invaded cells augmented from 40.27 ± 4.15 to 88.91 ± 6.76 after overexpression of PTBP1. In H1299 cells, the number of migrated cells increased from 68.24 ± 6.38 to 126.43 ± 5.28 and the number of invaded cells elevated from 54 ± 4.62 to 89.57 ± 8.39 following PTBP1 upregulation.

miR-133a Promoter Histone Has Significant Methylation Modifications

Aforementioned results have shown that miR-133a inhibited lung cancer growth and metastasis by binding to PTBP1, therefore we shifted our attention upon upstream of miR-133a. We first discovered via the UCSC browser website that miR-133a is located at chromosome 18, position chr18:21825698–21825785, and belongs to the same transcript as MIR133A1HG (Figure 6A and B). Moreover, the promoter sequence of miR-133a exhibits significant histone methylation modifications (Figure 6C), with the most pronounced levels of histone H3 lysine 4 trimethylation (H3K4me3) and H3K4me2 modifications. Thus, we further used anti-H3K4me3 or anti-H3K4me2 antibodies to detect the H3K4me3 or H3K4me2 modification levels of the miR-133a promoter in BEAS-2B cells and lung cancer cells. The H3K4me2 modification levels of miR-133a were significantly reduced in lung cancer cells (Figure 6D), while H3K4me3 levels were not significantly changed.

KDM5C Downregulates H3K4me2 Modification of the miR-133a Promoter Histone

It was noted by Glanzner et al that KDM5C mutation may inhibit H3K4me2 demethylation modifications of histones.[18] So, we speculated whether KDM5C

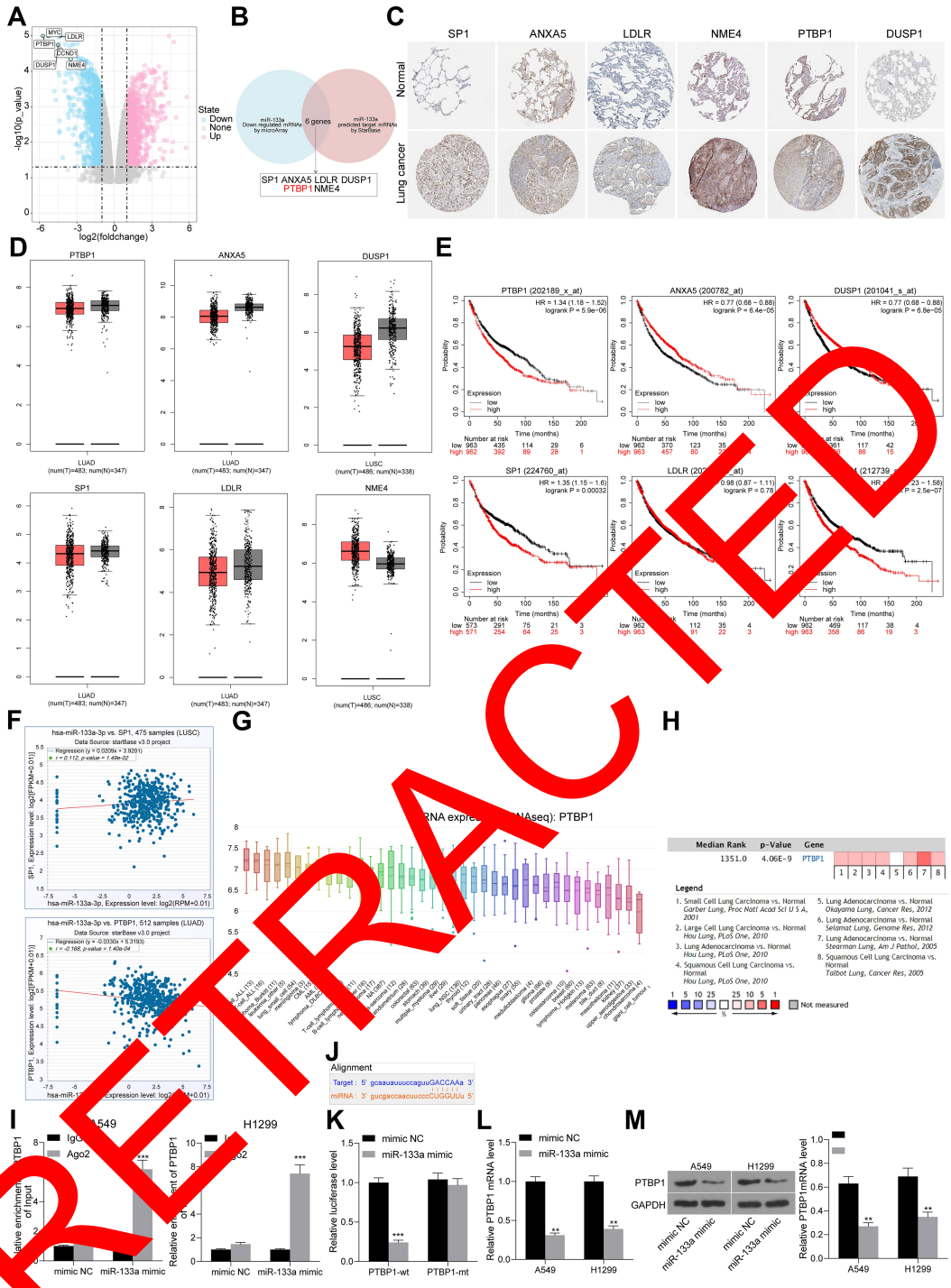

Figure 4 miR-133a targets and negatively regulates PTBP1. (**A**) volcano map showing differentially expressed mRNAs in A549 and H1299 cells with overexpression of miR-133a; (**B**) Venn map representing the target mRNAs predicted by the StarBASE website for miR-133a were screened against 186 differentially expressed mRNAs downregulated in the microarray results; (**C**) analysis of the staining intensity of PTPB1, SP1, ANXA5, DUSP1, LDLR, and NME4 in lung cancer or normal lung tissues via the HPA website (https://www.proteinatlas.org/); (**D**) expression of PTPB1, SP1, ANXA5, DUSP1, LDLR, and NME4 in lung cancer tissues and normal lung tissues from the TCGA-LUSC database; (**E**) Kaplan-Meier Plotter website analyzing the impact of PTPB1, SP1, ANXA5, DUSP1, LDLR, and NME4 on the prognosis of lung cancer patients; (**F**) Correlation of miR-133a with SP1 or PTBP1 analyzed in TCGA-LUAD database; (**G**) CCLE database predicting PTBP1 expression in various tumor cells; (**H**) PTBP1 expression in Garber Lung, Hou Lung, Okayama Lung, Selamat Lung, Stearman Lung, and Talbot Lung datasets in the Oncomine database; (**I**) RIP assay for miR-133a and PTBP1 binding relationship in A549 and H1299 cells; (**J**) predicted binding sites between miR-133a and PTBP1; (**K**) dual-luciferase assay detecting the binding relationship between miR-133a and PTBP1; (**L**) RT-qPCR assay for PTBP1 mRNA expression in A549 and H1299 cells; (**M**) Western blot assay for PTBP1 protein expression in A549 and H1299 cells. Data are presented as the mean ± SD. $^{**}p < 0.01$, $^{***}p < 0.001$. All results are from three independent experiment (**I**, **K**–**M**). Two-way ANOVA followed by Tukey post hoc test was utilized for multiple comparisons.

Abbreviations: miR, microRNA; PTBP1, polypyrimidine tract-binding protein 1; TCGA, The Cancer Genome Atlas; LUAD, lung adenocarcinoma; LUSC, lung squamous cell carcinoma; RT-qPCR, reverse transcription quantitative PCR; RIP, RNA immunoprecipitation; ANOVA, analysis of variance; SD, standard deviation.

Table 3 Differentially Expressed mRNAs in Both A549 and H1299 Cells Overexpressing miR-133a

Targets	Log Fold Change	*p* value	Targets	Log Fold Change	*p* value
CRNN	−7.94	0.000186192	HOXA10	2.5	0.007368496
HOXB7	3.28	0.000237485	CXCR2	−4.56	0.007387207
ANXA5	5.04	0.000578197	NUCB2	−3	0.007422249
SIM2	−2.77	0.000589149	CYP3A43	−1.87	0.007425284
CRISP3	−8.3	0.000760287	CRYL1	−1.9	0.007445407
PTBP1	7.2	0.001001076	EMP1	−2.73	0.00745166
HOXD11	3.53	0.00136076	TRAV12-2	−3.32	0.007594213
SP1	4.22	0.001867851	DNAH17	3.37	0.007709963
RHCG	−5.23	0.001977127	LDLR	2.43	0.007935064
ENDOU	−6.06	0.002064881	GPD1L	−2.13	0.00952764
TGM3	−5.36	0.002141302	PPL	−2.69	0.009867288
CLCA4	−5.53	0.002356211	GPX3	−3.48	0.009889021
MFHAS1	2.51	0.002410418	MSRA	−1.31	0.010380745
SERPINB1	−3.11	0.002431426	CRABP2	−2.77	0.010433333
C2orf54	−3.38	0.002583682	CLIC3	−5	0.010535843
ACOX3	−1.97	0.002721293	TFAP2B	−4.3	0.010706312
PARP12	1.84	0.003207005	FOXM1	2.03	0.011910802
RRAGD	−2.73	0.003698269	CYP3A5	−3.82	0.011969383
MYC	3.08	0.003803141	SERPINB3	4.07	0.012915799
SNAI2	2.71	0.004010746	CYP4B1	−3	0.013351085
ID4	−2.98	0.004718477	PLAGL1	−2.22	0.016161197
MAL	−5.48	0.004861099	MIND5B	−1.71	0.017476469
CES2	−2.39	0.004938248	ME4	4.49	0.017591122
SLURP1	−4.56	0.005070784	AP	2.42	0.017718714
BLNK	−2.74	0.005214198	AIM1	−1.88	0.017862179
HPGD	−4.42	0.005244754		−2.57	0.017956494
MET	1.63	0.005524125	KRT4	−6.14	0.018173813
CWH43	−4.2	0.005757	MCM2	2.21	0.018312306
CTSL	2.24	0.006496	ELOVL6	−2.23	0.018544204

similarly represses transcription by demethylation modification of the miR-133a promoter histone. To test our conjecture, we first constructed a luciferase reporter vector containing the miR-133a promoter and co-transfected into 293T cells with different doses of KDM5C overexpression vectors. We found that the luciferase activity was decreased as the doses of KDM5C overexpression vectors increased (Figure 7A). To further verify the binding relationship between KDM5C and the miR-133a promoter histone, we performed ChIP-qPCR experiments. We found significantly higher enrichment levels of the miR-133a promoter in the complexes pulled-down by the anti-KDM5C antibody than that by IgG (Figure 7B). Moreover, we further transfected the KDM5C overexpression plasmids into A549 and H1299 cells at different doses. A negative correlation was displayed between miR-133a expression in the cells and the doses of KDM5C overexpression vectors (Figure 7C). PTBP1, on the other hand, was positively correlated with the doses of KDM5C overexpression vectors (Figure 7D). Thus, we further analyzed the correlation between KDM5C and PTBP1 in the TCGA-LUAD and TCGA-LUSC databases, and we found that KDM5C was positively correlated with PTBP1 (Figure 7E and F). Subsequently, we further analyzed the expression of KDM5C in these databases. The expression of KDM5C in lung cancer tissues were higher than those in normal tissues in the half of the databases except in the databases of Garber Lung, Okayama Lung, and Talbot

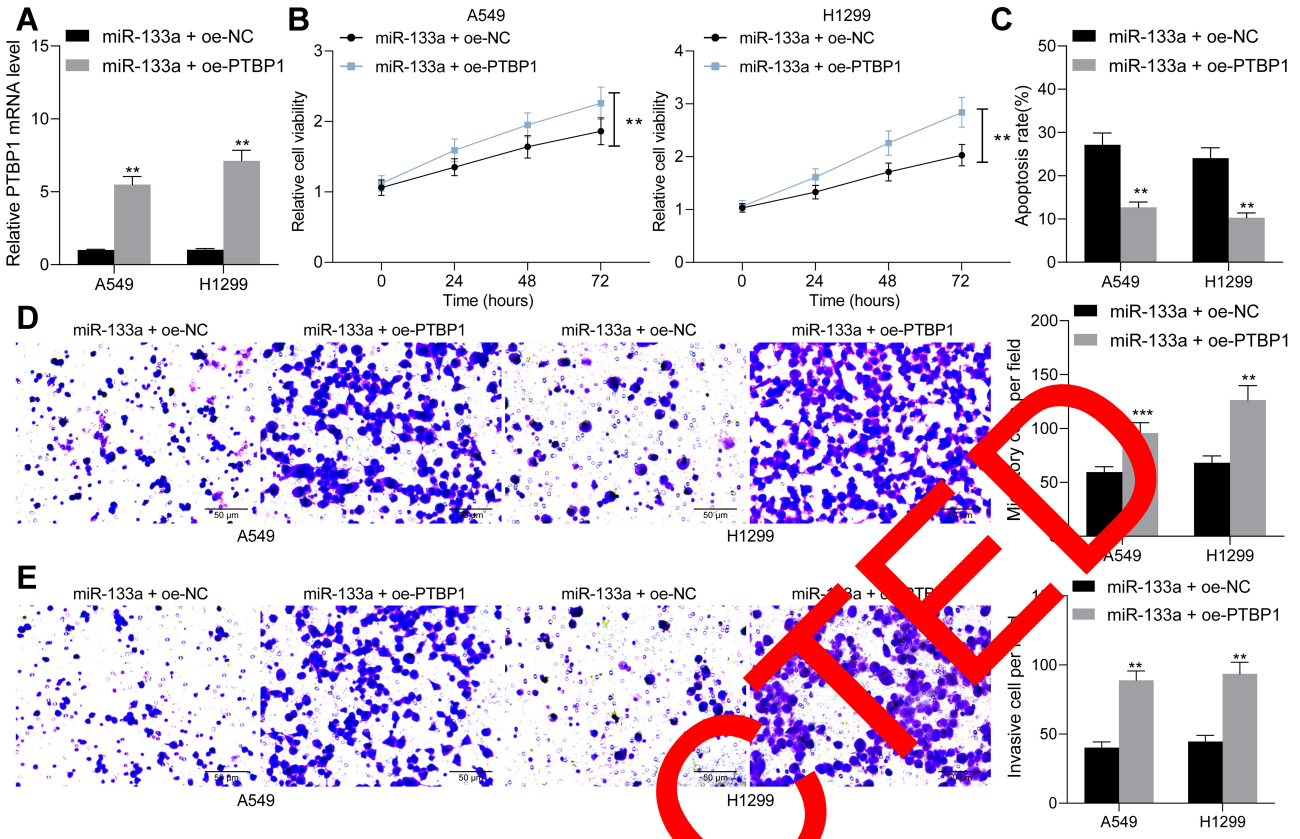

Figure 5 Overexpression of PTBP1 promotes growth and aggressiveness of lung cancer cells. oe-PTBP1 or oe-NC was transfected into lung cancer cells in the presence of miR-133a. (**A**) RT-qPCR detection of PTBP1 mRNA expression in A549 and H1299 after co-transfection; (**B**) CCK-8 assays for cell proliferation activity after co-transfection; (**C**) flow cytometry analysis of apoptotic proportions of cells after co-transfection; (**D**) Transwell experiments analysis of the migratory capacity of lung cancer cells after co-transfection; (**E**) Transwell experiments analysis of the invasive capacity of lung cancer cells after co-transfection. Data are presented as the mean ± SD. $^{**}p < 0.01$, $^{***}p < 0.001$. All results are from three independent experiments. Two-way ANOVA followed by Tukey post hoc test was utilized for multiple comparisons.
Abbreviations: miR, microRNA; oe, overexpression; PTBP1, polypyrimidine tract-binding protein 1; NC, negative control; RT-qPCR, reverse transcription quantitative PCR; CCK-8, cell counting kit-8; ANOVA, analysis of variance; SD, standard deviation.

Lung where there was no significant difference between the lung cancer tissues and normal tissues (Figure 7G).

Overexpression of KDM5C Promotes Malignant Biological Behavior of Lung Cancer Cells

To further validate the regulatory effect of KDM5C on the miR-133a/PTBP1 axis, thereby influencing lung cancer growth and metastasis, we further overexpressed KDM5C in cells stably overexpressing miR-133a. The expression of miR-133a decreased significantly after overexpression of KDM5C, while PTBP1 expression increased significantly (Figure 8A and B). Moreover, we found that the methylation modification level of miR-133a promoter was significantly reduced by 49.43 ± 5.07% in A549 cells and 57.79 ± 6.18% in H1299 cells after overexpression of KDM5C (Figure 8C). Overexpression of KDM5C was followed by significant augments in the cellular activity of A549 (28.03 ± 2.91%, 27.95 ± 3.11%, and 28.71 ± 2.79% by the 24th, 48th and 72nd h, respectively) and H1299 (24.26 ± 2.47%, 35.79 ± 4.28%, and 36.62 ± 3.75% by the 24th, 48th and 72nd h, respectively) (Figure 8D), accompanied by significant decreases in the number of apoptotic cells in A549 (from 26.83 ± 2.64% to 13.07 ± 1.31%) and H1299 (from 23.58 ± 2.36% to 9.87 ± 0.95%) cells (Figure 8E). We also found that A549 and H1299 cell migration and invasion were enhanced after overexpression of KDM5C. In A549 cells, the number of migrated cells increased from 51.27 ± 5.13 to 84.05 ± 9.55 and the number of invaded cells promoted from

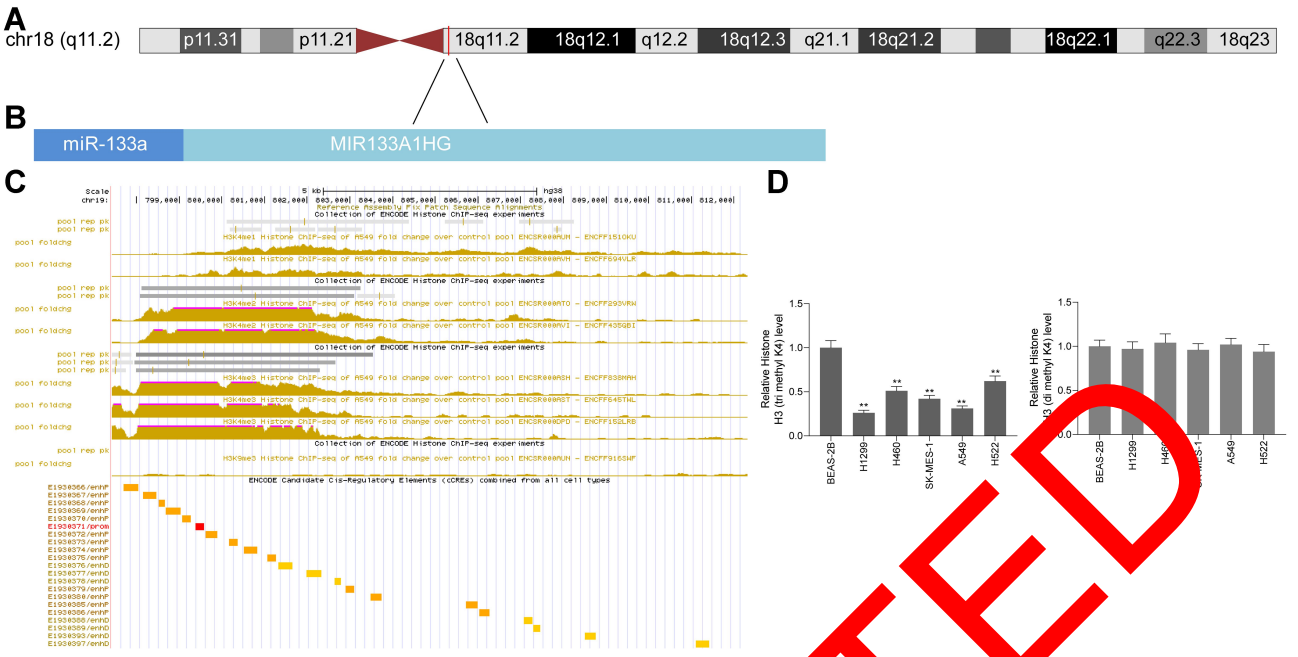

Figure 6 miR-133a promoter histone has significant methylation modifications. (**A**) the location of miR-133a on the chromosome predicted by UCSC website; (**B**) location of miR-133a in relation to its host gene; (**C**) UCSC website predicts histone methylation levels in the miR-133a promoter region; (**D**) ChIP-qPCR detection of H3K4me3 or H3K4me2 modification of the miR-133a promoter in BEAS-2B cells and lung cancer cells. Data are presented as the mean ± SD. $^{**}p < 0.01$. All results are from three independent experiment (**D**). Two-way ANOVA followed by Tukey post hoc test was utilized for multiple comparisons.
Abbreviations: miR, microRNA; ChIP, chromatin immunoprecipitation.

31.62 ± 3.49 to 72.04 ± 7.22 after overexpression of KDM5C. Consistently, in H1299 cells, the number of migrated cells elevated from 55.36 ± 6.54 to 121.47 ± 12.05, while the number of invaded cells increased from 33.83 ± 3.49 to 106.29 ± 11.63 (Figure 6F and G). The above results indicate that histone demethylase, KDM5C, promotes the expression of PTBP1 and thus the growth and metastasis of lung cancer through the demethylation modification of the miR-133a promoter histone.

Discussion

Various factors contributed to the dismal prognosis of patients with lung cancer involving late diagnosis and local and systematic metastasis.[19] As a consequence, metastasis continues to be a major obstacle in the effective treatment of lung cancer, and there is an urgency to identify molecular drivers to the invasiveness and metastasis in lung cancer. In present study, we identified that miR-133a was poorly expressed in lung tissues versus adjacent tissues, which predicts poor survival. Besides, miR-133a is involved in the phenotypic modulation of lung cancer cells by interacting with PTBP1. Moreover, we verified that KDM5C, an oncoprotein, accelerated lung cell growth and metastasis by modulating the miR-133a promoter histone methylation. These data indicate that KDM5C may function as an oncogene in lung cancer.

The tumor suppressor role of miR-133a has been well-established in osteosarcoma,[20] thyroid cancer,[21] as well as in gastric cancer.[22] More specifically, upregulation of miR-133a remarkably repressed cell growth, while induced apoptosis and caspase-3 activity in non-small cell lung cancer cells.[23] In consistence, our miRNA-based microarray on collected 37 pairs of lung cancer and adjacent tissues revealed that miR-133a was the most significantly downregulated miRNA in lung cancer. RT-qPCR results exhibited that miR-133a declined by 75.43 ± 5.97% in our collected lung cancer tissues relative to normal lung tissues. The subsequent bioinformatics inquiries further corroborated the association between miR-133a depletion and poor survival in lung cancer patients. In line with our findings, declines in miR-133a expression was found to share a close relation to hostile advancement in pancreatic cancer.[24] The anti-proliferatory (decreased by 20.51 ± 2.43% and 19.76 ± 1.85%, 70.42 ± 6.91% and 66.39 ±

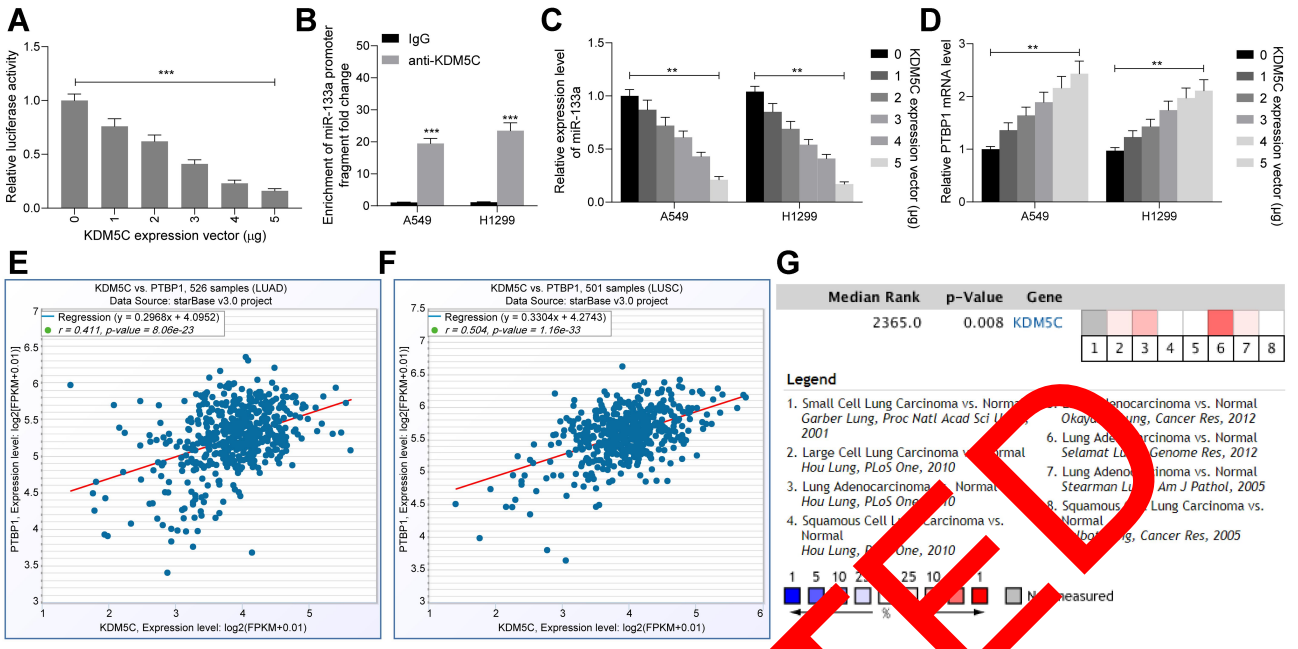

Figure 7 KDM5C reduces histone H3K4me2 demethylation of the miR-133a promoter. (**A**) luciferase reporter assay detecting the transcriptional binding of KDM5C to the miR-133a promoter; (**B**) binding of KDM5C to the miR-133a promoter histone verified using ChIP-qPCR experiments; (**C**) RT-qPCR analysis of the miR-133a expression in response to KDM5C overexpression vectors in A549 and H1299 cells; (**D**) RT-qPCR analysis of the expression of PTBP1 at mRNA level in response to KDM5C overexpression vectors in A549 and H1299 cells; (**E**) analysis of the correlation between KDM5C and PTBP1 in the TCGA-LUSC database; (**F**) analysis of the correlation between KDM5C and PTBP1 in the TCGA-LUAD database; (**G**) KDM5C expression in Garber Lung, Hou Lung, Okayama Lung, Selamat Lung, Stearman Lung, and Talbot Lung datasets in the Oncomine database. Data are presented as the mean ± SD. $^{**}p < 0.01$, $^{***}p < 0.001$. The results are from three independent experiment (**A**–**D**). Two-way ANOVA followed by Tukey post hoc test was utilized for multiple comparisons.

Abbreviations: miR, microRNA; KDM5C, lysine-specific histone demethylase 5C; ChIP, chromatin immunoprecipitation; RT-qPCR, reverse transcription quantitative PCR; TCGA, The Cancer Genome Atlas; LUAD, lung adenocarcinoma; LUSC, lung squamous cell carcinoma; PTBP1, polypyrimidine tract-binding protein 1; ANOVA, analysis of variance; SD, standard deviation.

6.53%, as well as 69.42 ± 7.68% and 66.66 ± 5.59% at the 24th, 48th h, and 72nd h, respectively), and invasive (from 96.55 ± 8.57 to 35.38 ± 4.19 and from 129.26 ± 11.12 to 45.63 ± 4.15), anti-migratory (from 136.25 ± 15.42 to 41.74 ± 5.26 and from 48.97 ± 16.27 to 53.36 ± 7.48) and pro-apoptotic (from 8.13 ± 0.82% to 26.45 ± 2.65% and from 3.93 ± 0.71% to 23.91 ± 2.36%) properties of miR-133a have been underscored in further functional experiments in A549 and H1299 cells. More importantly, the anti-metastatic role of miR-133a in vivo has also been highlighted in glioma[25] and gastric cancer,[26] which were largely consistent with our results.

Integrated bioinformatics prediction and mRNA-based microarray helped us to determine that PTBP1 was both a target of miR-133a and a downregulated mRNA in lung cancer cells overexpressing miR-133a. The involvement of PTBP1 in some cancers, such as colorectal cancer, breast cancer, glioma as well as pancreatic cancer has been reported.[27,28] For instance, PTBP1 knockdown led to constrained cell migration and invasion in addition to reduced metastasis in renal cell carcinoma.[29] Moreover, Kang et al provided evidence that miR-194 negatively regulated PTBP1 expression by binding to PTBP1 3′UTR in hepatocellular carcinoma.[30] Similarly, our RIP and dual-luciferase experiment verified the binding relation between PTBP1 and miR-133a in lung cancer. Furthermore, our observation from rescue experiments substantiated the tumor supporting role of PTBP1 in A549 and H1299 cells. Thereafter, we sought to explore the upstream mechanism of miR-133 downregulation in lung cancer.

Intriguingly, miR-133a-3p was validated to be knocked-down by DNA hypermethylation in breast cancer cells and tissue samples, which was in tight correlation with unsatisfactory prognosis of breast cancer patients.[31] Hence, we resorted to the UCSC browser website and noted that the promoter sequence of MIR133A1HG, which shares the same transcript with miR-133a, has distinct histone methylation modifications. In addition, it was noted by Glanzner et al that KDM5C

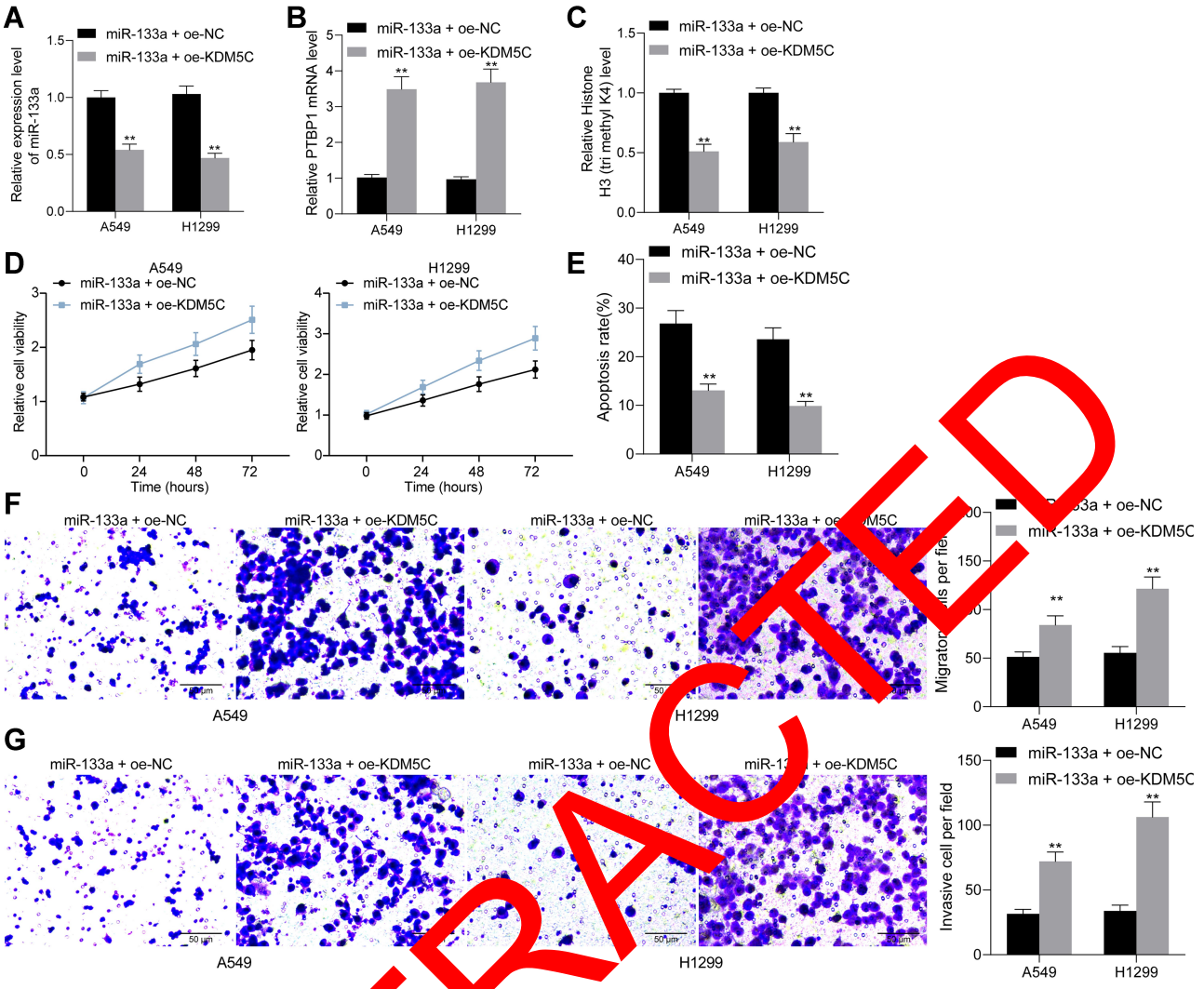

Figure 8 Overexpression of KDM5C promotes malignant biological behavior of lung cancer cells. oe-KDM5C or oe-NC was transfected into lung cancer cells in the presence of miR-133a. (**A**) RT-qPCR detection of miR-133a expression in A549 and H1299 after co-transfection; (**B**) RT-qPCR detection of PTBP1 mRNA expression in A549 and H1299 after co-transfection; (**C**) ChIP-seq detection of H3K4me3 modification level of miR-133a promoter after overexpression of KDM5C; (**D**) CCK-8 assays for cell proliferation activity after co-transfection; (**E**) flow cytometry analysis of apoptotic proportions of cells after co-transfection; (**F**) Transwell experiments analysis of the migratory capacity of lung cancer cells after co-transfection; (**G**) Transwell experiments analysis of the invasive capacity of lung cancer cells after co-transfection. Data are presented as the mean ± SD. **$P < 0.01$. All results are from three independent experiment. Two-way ANOVA followed by Tukey post hoc test was utilized for multiple comparisons.

Abbreviations: miR, microRNA; KDM5C, lysine-specific histone demethylase 5C; oe, overexpression; NC, negative control; RT-qPCR, reverse transcription quantitative PCR; ChIP, chromatin immunoprecipitation; CCK-8, cell counting kit-8; ANOVA, analysis of variance; SD, standard deviation.

mutation may inhibit H3K4me2 demethylation modifications of histones.[18] Thus, we speculated whether KDM5C similarly repressed transcription of miR-133a through demethylation modification of the its promoter histone. A series of regulatory experiments helped us confirm our speculation. We further tested the involvement of KDM5C in the miR-133a/PTBP1-mediated lung cancer malignant phenotype by rescue experiments. KDM5C, similar to PTBP1, plays a tumor-initiating role in lung cancer. In the same vein, the beneficial effects of KDM5C in sustaining cancer cell malignant aggressiveness has been witnessed in prostate cancer,[32] breast cancer,[33] gastric cancer[34] as well as hepatocellular carcinoma.[35]

Conclusion

In conclusion, the findings in this investigation elucidated that miR-133a, regulated by KDM5C, played a tumor suppressor role in lung cancer through regulation of PTBP1 (Figure 9). In spite of the fact that we acknowledged that miR-133a expression was mediated by KDM5C, and that miR-133a could suppress the

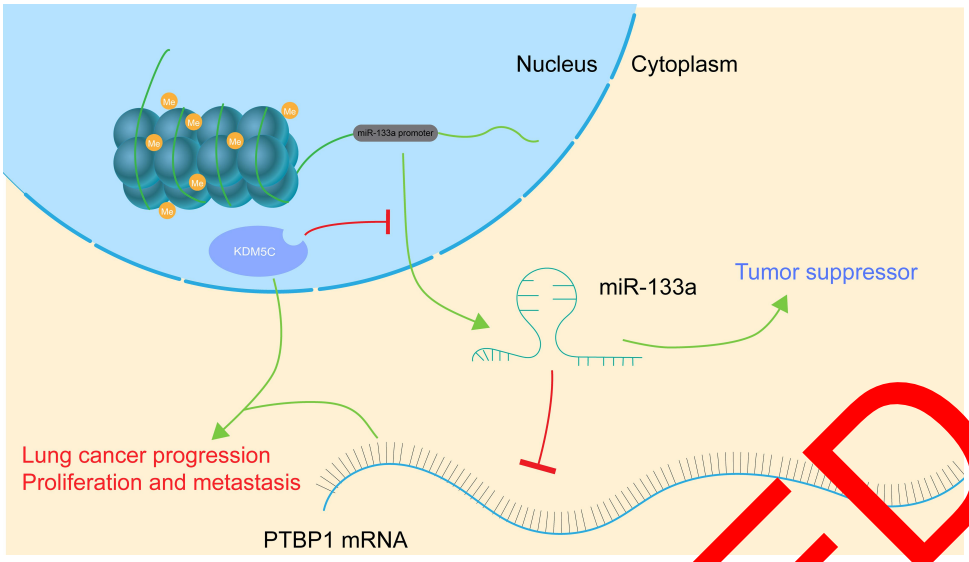

Figure 9 A working model for the role of KDM5C-targeted miR-133a in lung cancer progression and metastasis.
Abbreviations: miR, microRNA; KDM5C, lysine-specific histone demethylase 5C.

development and metastases of lung cancer by targeting PTBP1, there may be other upstream molecules and downstream targets of miR-133a affecting carcinogenesis of lung cancer. Further studies are essential to probe more mechanisms upstream and downstream of miR-133a in lung cancer.

Funding

There is no funding to report.

Disclosure

The authors report no conflicts of interest in this work.

References

1. de Groot PM, Wu CC, Carter BW, Munden RF. The epidemiology of lung cancer. *Transl Lung Cancer Res*. 2018;7(3):220–233. doi:10.21037/tlcr.2018.05.06
2. Bray F, Ferlay J, Soerjomataram I, Siegel RL, Torre LA, Jemal A. Global cancer statistics 2018: GLOBOCAN estimates of incidence and mortality worldwide for 36 cancers in 185 countries. *CA Cancer J Clin*. 2018;68(6):394–424. doi:10.3322/caac.21492
3. Santos RM, Moreno C, Zhang WC. Non-coding RNAs in lung tumor initiation and progression. *Int J Mol Sci*. 2020;21(8):2774. doi:10.3390/ijms21082774
4. Field JK, Oudkerk M, Pedersen JH, Duffy SW. Prospects for population screening and diagnosis of lung cancer. *Lancet*. 2013;382 (9893):732–741. doi:10.1016/S0140-6736(13)61614-1
5. Krol J, Loedige I, Filipowicz W. The widespread regulation of microRNA biogenesis, function and decay. *Nat Rev Genet*. 2010;11 (9):597–610. doi:10.1038/nrg2843
6. Nana-Sinkam SP, Croce CM. MicroRNA regulation of tumorigenesis, cancer progression and interpatient heterogeneity: towards clinical use. *Genome Biol*. 2014;15(9):445. doi:10.1186/s13059-014-0445-8
7. [illegible] ZQ, Wu CA, [illegible]ng YX. Prognostic value of microRNA-133a expression and its clinicopathologic significance in non-small cell lung cancer: a comprehensive study based on meta-analysis and the TCGA database. *Onkol Res Treat*. 2018;41(12):762–768. doi:10.1159/000492343
8. [illegible] WL, [illegible] H, Hu JJ, Wei XZ. Long noncoding RNA LINC00313 modulates papillary thyroid cancer tumorigenesis via sponging miR-4429. *Neoplasma*. 2018;65(6):933–942. doi:10.4149/neo_2018_180219N125
9. Xiao B, Liu H, Gu Z, Ji C. Expression of microRNA-133 inhibits epithelial-mesenchymal transition in lung cancer cells by directly targeting FOXQ1. *Arch Bronconeumol*. 2016;52(10):505–511. doi:10.1016/j.arbres.2015.10.016
10. Wang H, Zhang Y, Zhang Y, Liu W, Wang J. Cryptotanshinone inhibits lung cancer invasion via microRNA-133a/matrix metalloproteinase 14 regulation. *Oncol Lett*. 2019;18(3):2554–2559. doi:10.3892/ol.2019.10580
11. Berry WL, Janknecht R. KDM4/JMJD2 histone demethylases: epigenetic regulators in cancer cells. *Cancer Res*. 2013;73 (10):2936–2942. doi:10.1158/0008-5472.CAN-12-4300
12. Taylor-Papadimitriou J, Burchell J. JARID1/KDM5 demethylases as cancer targets? *Expert Opin Ther Targets*. 2017;21(1):5–7. doi:10.1080/14728222.2017.1263616
13. Garber ME, Troyanskaya OG, Schluens K, et al. Diversity of gene expression in adenocarcinoma of the lung. *Proc Natl Acad Sci U S A*. 2001;98(24):13784–13789. doi:10.1073/pnas.241500798
14. Hou J, Aerts J, den Hamer B, et al. Gene expression-based classification of non-small cell lung carcinomas and survival prediction. *PLoS One*. 2010;5(4):e10312. doi:10.1371/journal.pone.0010312
15. Okayama H, Kohno T, Ishii Y, et al. Identification of genes upregulated in ALK-positive and EGFR/KRAS/ALK-negative lung adenocarcinomas. *Cancer Res*. 2012;72(1):100–111. doi:10.1158/0008-5472.CAN-11-1403
16. Selamat SA, Chung BS, Girard L, et al. Genome-scale analysis of DNA methylation in lung adenocarcinoma and integration with mRNA expression. *Genome Res*. 2012;22(7):1197–1211. doi:10.1101/gr.132662.111

17. Talbot SG, Estilo C, Maghami E, et al. Gene expression profiling allows distinction between primary and metastatic squamous cell carcinomas in the lung. *Cancer Res*. 2005;65(8):3063–3071. doi:10.1158/0008-5472.CAN-04-1985
18. Glanzner WG, Gutierrez K, Rissi VB, et al. Histone lysine demethylases KDM5B and KDM5C modulate genome activation and stability in porcine embryos. *Front Cell Dev Biol*. 2020;8:151. doi:10.3389/fcell.2020.00151
19. Ashrafizadeh M, Najafi M, Makvandi P, Zarrabi A, Farkhondeh T, Samarghandian S. Versatile role of curcumin and its derivatives in lung cancer therapy. *J Cell Physiol*. 2020;235(12):9241–9268. doi:10.1002/jcp.29819
20. Qu Z, Li S. Long noncoding RNA LINC01278 favors the progression of osteosarcoma via modulating miR-133a-3p/PTHR1 signaling. *J Cell Physiol*. 2020. doi:10.1002/jcp.29582
21. Xia W, Jie W. ZEB1-AS1/miR-133a-3p/LPAR3/EGFR axis promotes the progression of thyroid cancer by regulating PI3K/AKT/mTOR pathway. *Cancer Cell Int*. 2020;20:94. doi:10.1186/s12935-020-1098-1
22. Hu ZH, Wang GJ, Li RX, et al. Upregulation of miR-133a-3p enhances bufothionine-induced gastric cancer cell death by modulating IGF1R/PI3K/Akt signal pathway mediated ER stress. *Life Sci*. 2020;259:118180. doi:10.1016/j.lfs.2020.118180
23. Guo N, Zhao Y, Zhang W, Li S, Li S, Yu J. MicroRNA-133a down-regulated EGFR expression in human non-small cell lung cancer cells via AKT/ERK signaling. *Oncol Lett*. 2018;16(5):6045–6050. doi:10.3892/ol.2018.9399
24. Wang Z. Diagnostic performance for declined microRNA-133a in pancreatic cancer. *J Cell Biochem*. 2019.
25. Luo C, Quan Z, Zhong B, et al. lncRNA XIST promotes glioma proliferation and metastasis through miR-133a/SOX4. *Exp Ther Med*. 2020;19(3):1641–1648. doi:10.3892/etm.2020.8426
26. Zhang X, Li Z, Xuan Z, et al. Novel role of miR-133a-3p in repressing gastric cancer growth and metastasis via blocking autophagy-mediated glutaminolysis. *J Exp Clin Cancer Res*. 2018;37(1):320. doi:10.1186/s13046-018-0993-y
27. Li C, Zhao Z, Zhou Z, Liu R. Linc-ROR confers gemcitabine resistance to pancreatic cancer cells via inducing autophagy and modulating the miR-124/PTBP1/PKM2 axis. *Cancer Chemother Pharmacol*. 2016;78(6):1199–1207. doi:10.1007/s00280-016-3178-4
28. Zhu W, Zhou BL, Rong LJ, et al. Roles of PTBP1 in alternative splicing, glycolysis, and oncogensis. *J Zhejiang Univ Sci B*. 2020;21(2):122–136. doi:10.1631/jzus.B1900422
29. Shan H, Hou P, Zhang M, et al. PTBP1 knockdown in renal cell carcinoma inhibits cell migration, invasion and angiogenesis in vitro and metastasis in vivo via the hypoxia inducible factor-1alpha pathway. *Int J Oncol*. 2018;52(5):1613–1622. doi:10.3892/ijo.2018.4296
30. Kang H, Heo S, Shin JJ, et al. A miR-194/PTBP1/CCND3 axis regulates tumor growth in human hepatocellular carcinoma. *J Pathol*. 2019;249(3):395–408. doi:10.1002/path.5325
31. Shi W, Tang T, Li X, et al. Methylation-mediated silencing of miR-133a-3p promotes breast cancer cell migration and stemness via miR-133a-3p/MAML1/DNMT3A positive feedback loop. *J Exp Clin Cancer Res*. 2019;38(1):42[illegible] doi:10.[illegible]86/s13046-[illegible]9-1400-z
32. Hong Z, Wu G, Xiang ZD [illegible]al. KDM5C is transcriptionally regulated by BRD4 and promotes castration-resistant prostate cancer cell proliferation by repressing PTEN. *Biomed Pharmacother*. 2019;114:108793. doi:10.10[illegible]biopha.2019.108793
33. Denis H, Van Grembergen O, [illegible]latte B[illegible]t al. MicroRNAs regulate KDM5 histone demethylases in breast cancer cells. *Mol Biosyst*. 2016;12(2):404–413. doi:10.1039/C5MB00513B
34. Xu L, Wu W, Cheng [illegible] et al. Enhancement of proliferation and invasion of gastric cancer cell by KDM5C via decrease in p53 expression. *Technol Cancer Res Treat*. 2017;16(2):141–149. doi:10.1177/1533034616629261
35. J[illegible]X, Jin S, Qu [illegible] et al. Lysine-specific demethylase 5C promotes hepatocellular carcinoma cell invasion through inhibition BMP7 expression. *BMC Cancer*. 2015;15:801. doi:10.1186/s12885-015-1798-4